

Numerical Simulation of Failure in Fiber Reinforced Composites

Original

Numerical Simulation of Failure in Fiber Reinforced Composites / Carrera, E., Kaleel, I., Petrolo, M.. - ELETTRONICO. - (2017). (XXIV International Conference of the Italian Association of Aeronautics and Astronautics, AIDAA 2017 Palermo-Enna (Italy) 18-22 September 2017).

Availability:

This version is available at: 11583/2684484 since: 2017-10-04T19:36:25Z

Publisher:

G. Davi and G. Tesoriere

Published

DOI:

Terms of use:

This article is made available under terms and conditions as specified in the corresponding bibliographic description in the repository

Publisher copyright

(Article begins on next page)

NUMERICAL SIMULATION OF FAILURE IN FIBER REINFORCED COMPOSITES

E. Carrera^{1*}, I. Kaleel¹, M. Petrolo¹

¹MUL² Group, Department of Mechanical and Aerospace Engineering, Politecnico di Torino, Corso Duca degli Abruzzi 24, 10129, Torino, Italy

[*erasmo.carrera@polito.it](mailto:erasmo.carrera@polito.it)

ABSTRACT

This paper presents numerical results concerning the failure analysis of fiber-reinforced composites. In particular, damage initiation and progressive failure are considered. The numerical framework is based on the CUF advanced structural models and the component-wise approach. Such models are employed at all scales. In other words, the same structural framework is employed for macro-, meso-, and microscales. Two approaches are assessed, including direct numerical simulations via micromechanical homogenization analysis and two-scale analysis. The results are compared with those from literature and attention is paid to the evaluation of the computational efficiency of the present numerical framework. In fact, 3D-like accuracy is sought with a reduced computational effort.

Keywords: Failure, Multiscale, Finite Element, CUF

1 INTRODUCTION

Over the years, the viability of virtual testing of heterogeneous material systems such as composite materials has significantly improved. Recent advances in computing capabilities have led to a variety of implementations for multi-scale analysis of heterogeneous systems. Micromechanics based failure analysis of composite structures is a competent tool to model damage progression as it can effectively capture explicit variation in constituent properties along with their non-linearities.

The paper presents an efficient finite element framework based on a class of refined finite beam models called Carrera Unified Formulation (CUF) for failure analysis in fiber-reinforced structures [1]. The energy based crack band theory (CBT) is implemented within the framework to predict the damage propagation in individual constituents [2,3]. The micromechanics framework is integrated into two-scale progressive failure analysis framework. The efficiency of the framework is derived from the ability of CUF models to provide accurate three-dimensional displacement and stress fields at a reduced computational cost (approximately one order of magnitude of degrees of freedom less as compared to standard 3D brick elements).

2 CARRERA UNIFIED FORMULATION

2.1 One-dimensional unified formulation

The coordinate system adopted is illustrated in Fig. 1. The longitudinal axis of the beam coincides with the y-axis of the coordinate system ($0 \leq y \leq L$) and the cross-section Ω is overlaid on the x-z plane.

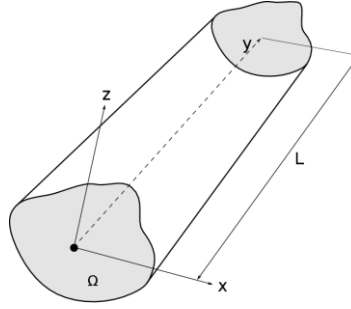


Figure 1: Coordinate system for the 1D beam

Carrera Unified formulation (CUF) expresses the displacement field as an expansion of generic cross-section function $F_\tau(x, z)$ with the displacement $\mathbf{u}_\tau(y)$

$$\mathbf{u}(x, y, z; t) = \{u_x \ u_y \ u_z\}^T \quad (1)$$

$$\mathbf{u}(x, y, z; t) = F_\tau(x, z)\mathbf{u}_\tau(y; t), \quad \tau = 1, 2, \dots, M$$

where T is the number of terms in cross-section expansion function F_τ . The class of 1D CUF model adopted is based on the choice of F_τ . Two classes of cross-section expansion functions are introduced within the context of this report: (1) Taylor Expansion (TE) and (2) Lagrange Expansion (LE) [1]. TE 1D models are based on the polynomial expansion of the kind $x^i z^j$, as cross section function F_τ , where i and j are positive integers [4]. LE 1D models are formulated using Lagrange polynomials as cross-section function F_τ [5]. These expansion functions consist of purely displacement values whereas 1D TE models are characterized with displacement and N -order derivatives of the displacements. Please refer to book by Carrera et al. for a comprehensive review on the CUF models [1].

2.2 Finite element formulation

By adopting the conventional FE approach to discretize the beam along the y -axis, the displacement vector \mathbf{u} can be defined as

$$\mathbf{u}(x, y, z; t) = F_\tau(x, z)N_i(y)\mathbf{u}_{\tau i}, \quad \tau = 1, 2, \dots, M; \quad i = 1, \dots, p + 1 \quad (2)$$

where N_i is the beam shape function of order p and $\mathbf{u}_{\tau i}$ is the nodal displacement vector. The principle of virtual displacement holds

$$\delta L_{int} = \delta L_{ext} - \delta L_{ine} \quad (3)$$

where L_{int} stands for internal strain energy, L_{ext} stands for work done by the external loads and L_{ine} is the work done to inertial loading and δ stands for virtual variation. The stiffness and mass matrices and loading vector is obtained via manipulation of Eqn. (3). For further reading on formulation and assembly of global matrices, refer to book by Carrera et al [1].

3 COMPONENT-WISE MICROMECHANICAL FRAMEWORK AND CONSTITUTIVE MODELING OF DAMAGE

Within the Component-Wise micromechanical framework, the RVE is modelled as a beam structure with the cross-section discretized into an arbitrary number of Lagrange elements along

the x_2 - x_3 plane as illustrated in Fig. 3 [6]. The cross-section of the RVE is discretized into multiple CW Lagrange elements with different constitutive properties. This enables the displacement and traction continuity across the interfaces of the different constituents. The cross-section extends along the span of the beam in the x_1 direction. The beam is modelled using B4 elements (cubic interpolation). To remain consistent with periodic assumptions of the RVE, periodic boundary conditions (PBCs) need to be applied. A detailed description of the PBC implementation for CUF elements can be found in [6].

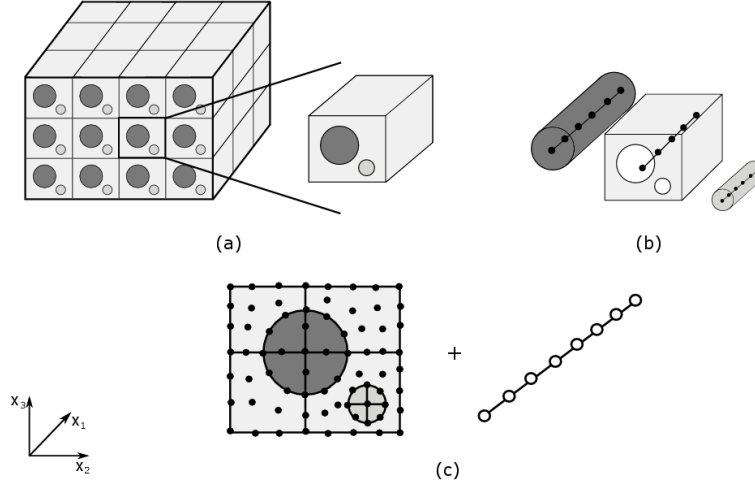


Figure 2: an illustration of a component-wise modeling of composite microstructure with arbitrary constituents

3.1 Smearred crack band model

The micromechanical analysis yields accurate three-dimensional strain and stress fields. These local fields are used to govern the progressive damage evolution within the RVE. The smearred crack band model is implemented within the CUF-CW micromechanical framework [2,3]. The smearred crack band model captures the behaviour of numerous micro-cracks formed in a given region and the energy dissipated during the formation of the crack band is smearred over the width within the finite element. The dissipated energy is related to the material fracture toughness. The fracture toughness G_c of the material is computed by the area under the traction-separation law, which governs the cohesive behaviour of the crack propagation.

3.1.1 Mode I crack under tensile principal stress

When the principal stress with the largest magnitude is tensile in nature, it is assumed that the crack orients such that it is subjected to the pure mode I loading. The characteristic length l_c is computed as the dimension of the finite volume running parallel to \mathbf{n}_1 . Maximum stress criterion is used to determine the crack band initiation [7]:

$$\frac{\sigma_1^m}{\sigma_c^m} = 1 \quad (4)$$

where σ_c^m is the cohesive strength of the crack band. Upon initiation, the orientation of the crack band is fixed. The post-peak softening slope E_{IT} and the strain at failure is computed using the characteristic length l_c and matrix fracture toughness G_c [2]

$$\varepsilon_f = \frac{2G_c}{\sigma_c^m l_c} ; E_{IT} = \left(\frac{1}{E_m^0} - \frac{\varepsilon_f}{\sigma_c^m} \right)^{-1} \quad (5)$$

composite. The strength of an un-notched composite specimen is discussed in the second numerical result.

5.1 Micromechanical progressive Failure analysis of randomly distributed fiber-reinforced composite

Failure evolution in a randomly distributed fiber composite RVE under transverse tension is investigated. The failure mechanism is characterized to be brittle in nature accompanied with matrix cracking. In order to simulate the failure mode, a randomly distributed fiber composite RVE is developed in the CUF-CW micromechanics module as depicted in Fig. 5 [8]. The cross-section is modelled using 265 L9 elements as depicted in Fig. 5 and the beam is discretised using 2 B4 elements with the length of 3mm. The total degrees of freedom of the problem amounts to a sparse system of 19,080.

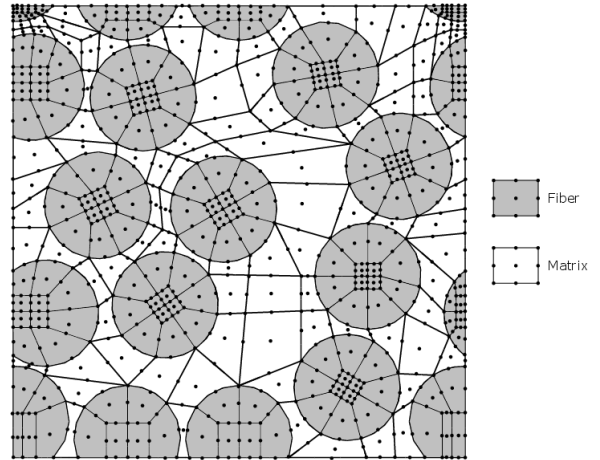


Figure 4: CW discretization of the cross-section of RVE with 13 randomly distributed fibers

A similar RVE model is developed using 3D brick element using 24,765 brick elements with total degrees of freedom of 91,305. Fiber is assumed to be linearly isotropic in nature. Matrix exhibit linear isotropic behaviour coupled with crack band model for postpeak softening. The material properties for fiber (Silenka E-glass fiber) and MY750/HY917/DY063 epoxy matrix is tabulated in Table 1 [8].

A global strain of 0.004 was applied along the transverse direction (x_2) of RVE. Figure 6 depicts the transverse stress versus transverse strain for randomly distributed fiber composite RVE under transverse tension. The contour plots for damage progression at various strains from transverse loading of RVE using CUF-CW and FEM 3D are depicted in Fig. 5.

Following observations can be made:

1. The ultimate global transverse stress computed using CUF-CW was 46.15 MPa at a strain of 0.0031, whereas the analogous FEM 3D model prediction amounted to 51.11 MPa at a strain of 0.0029.
2. From the damage contours (see Fig. 5), it can be postulated that CUF-CW and FEM 3D provide comparable quantitative results for the applied global transverse strain and match well with crack paths observed in experiments.

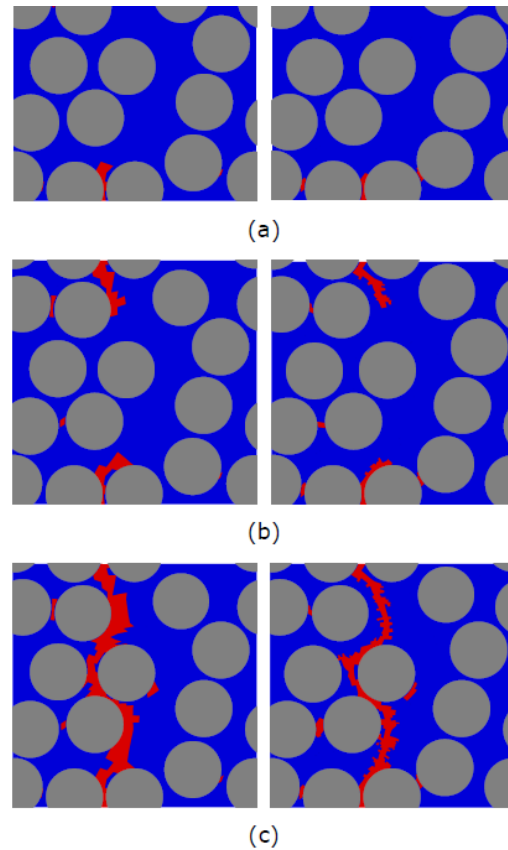


Figure 5: Damage progression in the randomly distributed fiber composite under transverse tension at global strains (a) 0.00275, (b) 0.0035 and (c) 0.004 (gray: fiber, blue: undamaged matrix, red: damaged matrix)

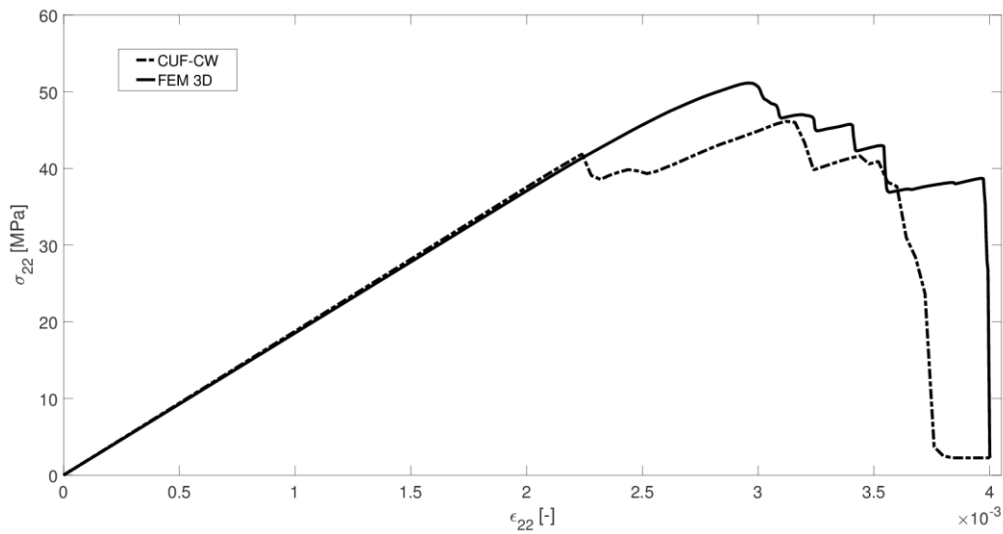


Figure 6: Transverse tensile stress versus transverse tensile strain for randomly distributed fiber composite under transverse tension

5.2 Two-scale progressive failure analysis of un-notched and notched fiber reinforced composite

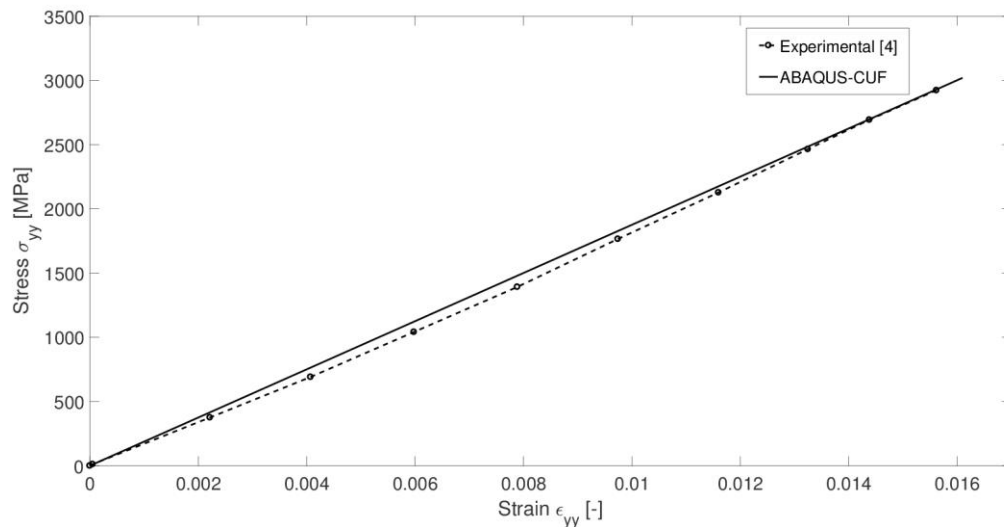


Figure 7: Uniaxial stress-strain curve for laminates $[0]_8$

An unnotched $[0]_8$ coupon under uniaxial tension is simulated. A triply periodic RVE (see Fig. 1) is used for analysing the composite coupon. The volume fraction of the RVE is 65% and it is made of IM7/977-3 material configuration [3]. The structural coupon was modelled in ABAQUS using C3D8 brick element and CUF-RVE micromechanical module is called at every gauss point for material response. The stress-strain response for a $[0]_8$ laminate is presented in Fig. 5.

6 CONCLUSION

Progressive failure analysis of fiber-reinforced composite using the newly developed framework based on refined beam models is successfully undertaken. The smeared crack band model is implemented within the CUF-CW micromechanics framework to simulate failure progression within an RVE containing 13 randomly distributed fibers under transverse tension loading conditions. The predicted failure modes using CUF-CW corresponds well with the analogous FEM 3D model and observations made in the experiments. The efficiency of the CUF-CW models in comparison to the standard FEM 3D model is highlighted.

A novel micromechanics-based two-scale analysis for progressive damage analysis of composite is also presented. The micromechanics module integrated into the framework for undertaking progressive failure analysis. The efficiency of CUF beam models to produce an accurate displacement and stress fields is exploited for micromechanical analysis. Result for an unnotched [0]_s coupon under uni-axial tension is presented. The result is validated against experimental data.

Future work includes exploring damage progression within RVE under compressive and shear loading conditions. Exploiting the two-scale progressive failure analysis framework to estimate stiffness and strength of notched and unnotched composite specimen shall also be undertaken.

7 ACKNOWLEDGEMENTS

This research work has been carried out within the project FULLCOMP (FULLy analysis, design, manufacturing, and health monitoring of COMPOSITE structures), funded by the European Union Horizon 2020 Research and Innovation program under the Marie Skłodowska-Curie grant agreement No. 642121.

REFERENCES

- [1] Carrera, E., Cinefra, M., Zappino, E., and Petrolo, M. “Finite Element Analysis of Structures Through Unified Formulation”, John Wiley & Sons Ltd. (2014).
- [2] Z. Bazant, and B. H. Oh. “Crack band theory of concrete”. *Materials and Structures*, **16**, pp. 155–177 (1983).
- [3] D. K. Patel, A. D. Hasanyan, and A. M. Waas. N -layer concentric cylinder model (Ncyl): An extended micromechanics-based multiscale model for nonlinear composites. *Acta Mechanica*, **228**(1), Pp. 275–306 (2017).
- [4] E. Carrera, G. Giunta. Refined beam theories based on a unified formulation. *International Journal of Applied Mechanics*, **02**(01), pp. 117-143 (2010).
- [5] E. Carrera, M. Petrolo. Refined beam elements with only displacement variables and plate/shell capabilities. *Meccanica* **47** (3), pp. 537-556 (2012).
- [6] I. Kaleel, M. Petrolo, E. Carrera, and A. M. Waas. Computationally efficient, high-fidelity micromechanics framework using refined beam models. *Submitted* (2017).
- [7] T. Tay, G. Liu, V. Tan, X. Sun, and D. Pham. “Progressive failure analysis of composites”. *Journal of Composite Materials*, **42**(18), pp. 1921–1966 (2008).

- [8] E. J. Pineda, B. A. Bednarczyk, A. M. Waas, and S. M. Arnold. “Progressive failure of a unidirectional fiber-reinforced composite using the method of cells: Discretization objective computational results”. *International Journal of Solids and Structures*, **50**(9), pp. 1203–1216 (2013).